

# Segmenting melanoma Lesion using Single Shot Detector (SSD) and Level Set Segmentation Technique

Faaiza Rashid

Deptt. of Computer Science  
University of Engineering & Technology  
Taxila, Pakistan  
faazarashid35@gmail.com

Aun Irtaza

Deptt. of Computer Science  
University of Engineering & Technology  
Taxila, Pakistan  
aun.irtaza@uettaxila.edu.pk

Nudrat Nida

Deptt. of Computer Engineering  
University of Engineering & Technology  
Taxila, Pakistan  
16F-PHD-CP-53@uettaxila.edu.pk

Ali Javed

Deptt. of Software Engineering  
University of Engineering & Technology  
Taxila, Pakistan  
ali.javed@uettaxila.edu.pk

Hafiz Malik

Deptt. of Electrical & Computer Engg.  
University of Michigan-Dearborn  
Dearborn, MI, USA  
hafiz@umich.edu

Khalid Mahmood Malik

Deptt. of Computer Science & Engg.  
Oakland University  
Rochester, MI, USA  
mahmood@oakland.edu

**Abstract**—Melanoma is a lethal type of skin cancer that originates from melanocytes cells of skin and it is responsible of several deaths annually due to exposure of ultraviolet radiations. Early diagnosis and proper treatment of melanoma significantly improves the patient's survival rate. In the computer aided diagnosis, the automatic segmentation is first step in early and accurate diagnosis of the Melanoma lesion area. However, the presence of natural or clinical artifacts hinders the precise lesion segmentation. The goal of our work is to establish a novel pipeline that automatically pre-process, localize and then segment the melanoma lesion precisely and improve its segmentation accuracy. In our proposed method, dermoscopic images are segmented in three steps: 1. Preprocessing using morphological operations to remove hair. 2. Localization of melanoma lesion by utilizing a deep convolutional neural network named as Single-Shot Detection (SSD) network, 3. Segmentation using level set algorithm. The proposed approach was evaluated on ISBI 2016 challenge dataset (Skin Lesion Analysis Towards Melanoma Detection Challenge Dataset). On ISIC 2016, our method achieved an average of Jc, Di and Ac as 0.82, 0.901 and 0.90 respectively. The results of the segmentation are also compared with the state-of-the-art methods to justify the effectiveness of the proposed approach.

**Index Terms**—SSD, CAD tool, Deep learning, Melanoma localization, level-set segmentation.

## I. INTRODUCTION

Among all types of skin cancer, Melanoma accounts for less than 5% but it is the most dangerous form leading to the vast majority of deaths/higher death rates every year [1]. In the United States alone Melanoma affect an estimated 96,480 people leading to 7,230 deaths in 2019 [2]. One of the major cause of melanoma skin cancer is due to overexposure to ultraviolet radiation coming from sunlight as well as artificial sources such as tanning devices [2]. In more than 95% of cases, Melanoma can be curable if it is treated properly and diagnosed in its early stages that significantly improve the

patient's survival rate [3]. However, due to visual similarity of melanoma lesion with normal skin, detection of Melanoma skin cancer is very challenging task through naked eyes that results in late diagnosis.

Hence, over the years, many methods have been utilized to determine the melanoma and one of them is dermoscopy. The dermoscopy is non-invasive imaging tool for an in vivo inspection that acquires a magnified and an illuminated image by enhancing the visibility of spots and morphological features on skin [4]. Thus this is very helpful in accessing the melanoma lesion at earlier stages and get higher accuracy rates than evaluation through naked eyes. These dermoscopy procedures are very helpful in diagnosis of melanoma skin cancer patients but there are some issues that should be considered. Firstly, the procedures are very time consuming so it would not be capable to examine the lesions at large scale and earlier stages. Secondly, in some areas like rural area there are limited number of dermatologists and inexperienced clinicians experts who have very little knowledge about the dermoscopy procedures. Also, the interpretation made by even well trained dermatologists show variability and produce different results while examining the same lesions. Thus, in order to overcome these difficulties there is a dire need to develop computer aided diagnosis (CAD) systems that may assist dermatologists in timely detection of Melanoma skin cancer and reduce the morality rate.

The CAD systems mainly constitute of four steps: pre-processing, segmentation, feature extraction and classification. In the computerized analysis, the automated lesion segmentation is an essential first step before classification which allows the extraction of the lesion area from healthy skin of dermoscopic images. The automatic lesion segmentation in dermoscopic images is very challenging because of the

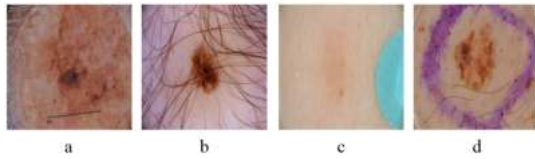


Fig. 1. Some challenging cases for the segmentation task in ISIC 2016 images. (a) ruler marker (b) hair (c) poor contrast and color chart (d) ink marking.

great variety of lesion size, location, arbitrary shape, and variation in color over different patients. Besides, the presence of clinical or natural artifacts such as blood vessels, hair, and air or gel bubbles also cause difficulties to the segmentation process. Moreover, the low contrast between the lesion and the surrounding textures also hinders the precise automatic lesion segmentation. Figure 1 shows some artifacts within dermoscopy images of ISIC 2016 challenge dataset.

The traditional techniques for segmenting Melanoma lesion from healthy skin are Otsu's thresholding [5], adaptive thresholding [6], iterative stochastic region merging [7] and level set [8]. Thresholding based techniques suffer from under or over segmentation due to variation in color, illumination and chrominance within the dermoscopic images. In [5], Otsu's thresholding produced good results but it has a limitation that the boundary of segmented lesion is irregular and the size of the segmented lesion is smaller as compared to its original size due to vague boundary of lesion. In an active contour based model, the initial curve moves towards the ROI boundary through deformation. The deformable models can be classified as a parametric and geometric model. The parametric models have some limitations that the initial curve must be near the ROI boundary and also these models face difficulty in dealing boundaries with very large curvature. While, Level set [8] and Chan-Vese's methods [9], also known as active contour without edges, are the examples of geometric models. To overcome the limitations of traditional parametric models level set method are used which can easily control the topological changes during curve evolution [8]. As, Level set function implicitly track the curve evolution that finds the position of the pixel within an image very easily, whether it is inside, outside or on the curve. The level set can easily compute the geometric properties of the curve and suitable for melanoma segmentation.

Recently, deep neural networks have shown remarkable advances in computer vision to solve problems like object localization, detection, and segmentation. Deep learning based on a convolutional neural networks has a potential to automatically learn prominent features from an image rather than handcrafted features leading to a better improvement in performance [10]. In recent works, many researchers have applied these deep learning based methods in medical analysis applications for Melanoma detection [11] and segmentation [12] which shows the significant improvement in performance over traditional based methods due to its discriminative ability of learning prominent features. Many object localization algorithms based on deep learning generate region proposal such

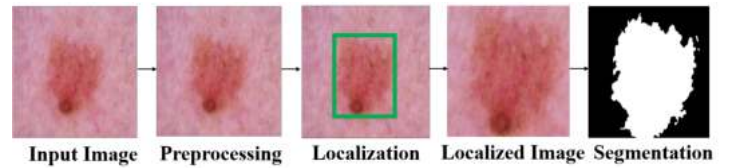


Fig. 2. Architecture of proposed methodology for detection and segmentation of Melanoma lesion region.

as, RCNN, R-FCN, which makes the networks very complex and slow and computationally expensive. In contrast to that, SSD [13] is a single forward network that avoids the region proposal generation making the network structure simple which further improves the speed and accuracy. Therefore, in this research paper, we are presenting melanoma segmentation using SSD and level-set segmentation.

## II. PROPOSED METHODOLOGY

### A. System Review

In our proposed approach pre-processing is the primary step to exclude artifacts such as hair, tiny blood vessels, and ruler markings from skin images to improve the segmentation of melanoma lesion. After pre-processing, localization of skin lesion was employed through SSD network followed by level set segmentation to precisely segment out the boundaries of melanoma. The proposed methodology is elaborated in Figure 2.

### B. Skin Enhancement

The existence of hair and presence of artifacts like ruler markings and blood vessels hinders the precise melanoma segmentation. Thus morphological closing opening operation was used to eliminate thick or thin hair and clinical ruler marks using line structuring elements  $S_1$  from a given input image. The closing operation used two different line structuring element at different directions to performs dilation operation followed by erosion operation on an input dermoscopic images. The reason behind using two different line structuring element  $90^\circ$  and  $180^\circ$  is to eliminate both vertical and horizontal hair respectively. It is defined as:

$$I_{mor}(x, y) = (I(x, y) \oplus L) \ominus L \quad (1)$$

Where L is the line structuring element at  $90^\circ$  and  $180^\circ$  that constitute 10 pixels for every pixel. The final morphed image  $I_f(x, y)$  overcame the natural or clinical artifacts including hair, and ruler mark. From Figure 3, we can be noted that resultant images after skin enhancement is visually improved and remove artifacts like thick hair, thin hair, ruler marking etc.

### C. Melanoma Detection using SSD

For Melanoma lesion detection we employed the deep CNN based Single Shot Detector [13] that sum-up all computation in only one forward pass network. The main idea of SSD network is to make predictions from several features maps,



Fig. 3. Example of Hair and Ruler Marking Removed Images.

where each feature map is directed for detecting objects at multiple scales followed by non-maximum suppression to generate final detections. Unlike RCNN, Faster RCNN and other object detection models SSD network directly compute set of boundary boxes score and confidence score by eliminating region proposal stage. As, SSD does not require an intermediate region proposal step, therefore SSD holds low complexity overhead and real-time processing for Melanoma lesion detection. Due to these performance benefits, we opted SSD for the localization of melanoma lesion.

For prediction task, from all location of the multiple feature maps SSD uses the K default boundary box rather than predicting the boundary box directly. The default boxes are associated with multi scales and aspect ratio that gives information of the lesion at multiple scale.

The predicted boundary boxes  $bbox_{pt}$  are integrated and matched with ground truth boundary boxes  $bbox_{gt}$  using IOU overlapping criteria. The IOU value is computed as shown in (eq. 2). For our Melanoma lesion detection model, we have chosen the IOU threshold value as 0.6 for precise detection. If the IOU score is greater than 0.6 then it detects the region as Melanoma lesion otherwise it is considered a healthy skin region.

$$IOU = \frac{bbox_{pt} \cap bbox_{gt}}{bbox_{pt} \cup bbox_{gt}} \quad (2)$$

1) *Training parameters for SSD*: We used the object-detection model which was pre-trained on the COCO dataset. By means of transfer learning we fine tune the SSD model on ISIC 2016 challenge dataset for precise localization of Melanoma. RMSprop [14] was used as the optimization function with 0.004 learning rate, a decaying factor of 0.95 and batch size 24.

#### D. Melanoma segmentation using Level Set

For segmentation phase, we applied the Chan-Vese's model for level set method based on curve evolution formulation [7]. Initially region  $\Omega$  is divided into two sub-regions, foreground region  $\Omega_{in} = \{\phi(x) > 0\}$  and background region  $\Omega_{out} = \{\phi(x) < 0\}$  by a contour  $C = \{\phi(x) = 0\}$ . In the proposed model an image  $I_f(x, y)$  is segmented using a level

set function  $\phi$ . The chan-veese model relies on minimization of intensity-based energy  $E$  functional that is defined as:

$$E = \int_{\Omega_{in}} |I_f(x, y) - c_1|^2 dx + \int_{\Omega_{out}} |I_f(x, y) - c_2|^2 dx + |C| \quad (3)$$

where  $|C|$  expresses the length of the segmenting contour of ROI. However, the values  $c_1$  and  $c_2$  denote the average intensities values of ROI and background regions indicated as following:

$$c_1 = \frac{1}{|\Omega_{in}|} \int_{\Omega_{in}} I_f(x, y) dx \quad (4)$$

$$c_2 = \frac{1}{|\Omega_{out}|} \int_{\Omega_{out}} I_f(x, y) dx \quad (5)$$

Therefore, by using the functional energy  $E$  in equation 4 the local minimization is done through gradient descent. Afterwards the regularized minimization problem can be changed into an evolutionary partial differential equation (PDE) on the function  $\phi$ . Hence the segmentation is achieved by computing the level set function and the constants  $c_1$  and  $c_2$  that minimizes the energy. The chan-veese level based method is robust against noise and can be applied to many medical segmentation problems containing artifacts.

### III. EXPERIMENTS AND RESULTS

#### A. Dataset

For the performance evaluation, the publicly available datasets ISBI 2016 was used to examine the performance of our proposed approach. The datasets was provided by International Skin Imaging Collaboration (ISIC) in 2016. For the segmentation task, ISIC 2016 provides 900 images for training and 379 images for testing along with their ground truth images.

#### B. Results and discussion

This section present the results obtained and examine the performance of the proposed approach on ISIC 2016 dataset.

1) *Melanoma detection*: After skin refinement phase, the enhanced dermoscopic images were further processed for detection of Melanoma. The results of a few best scoring Melanoma detection lesion are shown in Figure. 4. It is notable from Fig. 4 that SSD detected the Melanoma lesion accurately, and automatically eliminates the artifacts such as ruler markings, color calibration charts, and dark background frames. The performance of SSD VGG was evaluated in Table. 1. During these experiments, on ISIC 2016 SSD VGG performed 94% precision and has a recall of 83%.

TABLE I  
PERFORMANCE OF SSD (VGG AS BASE NETWORK) IN TERMS OF  
PRECISION AND RECALL

Dataset	Method	Precision	Recall
ISIC 2016	SSD (VGG)	94%	83%

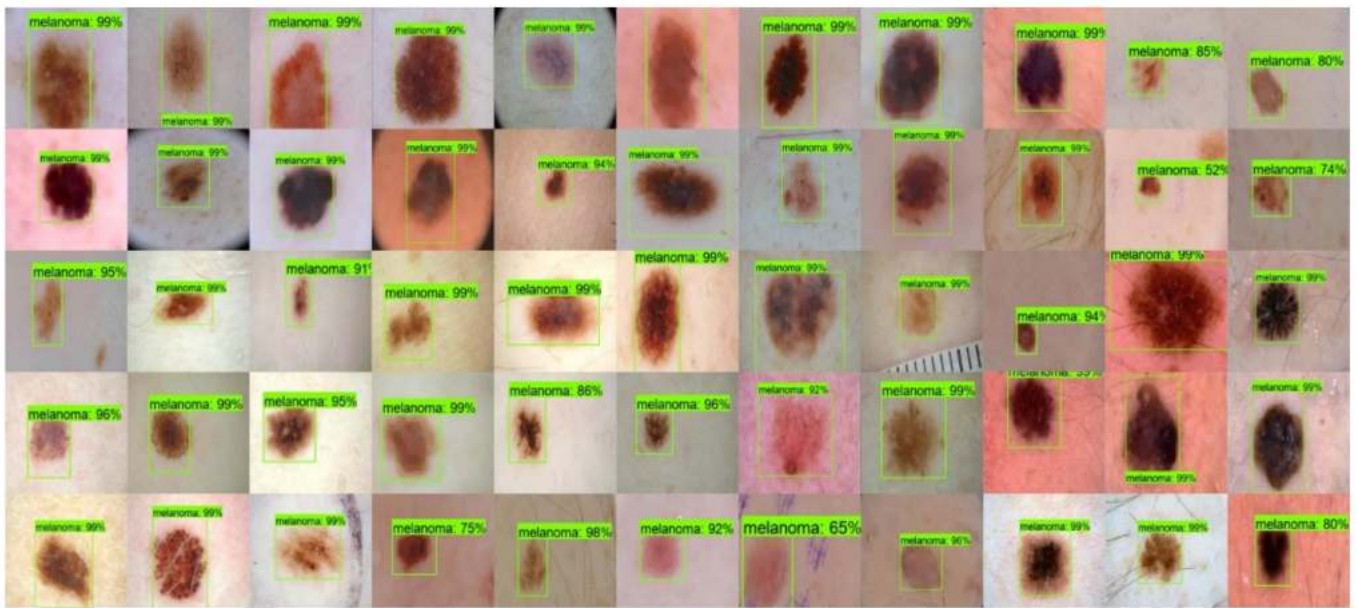


Fig. 4. Samples of some best scoring detections on ISIC 2016 dataset.

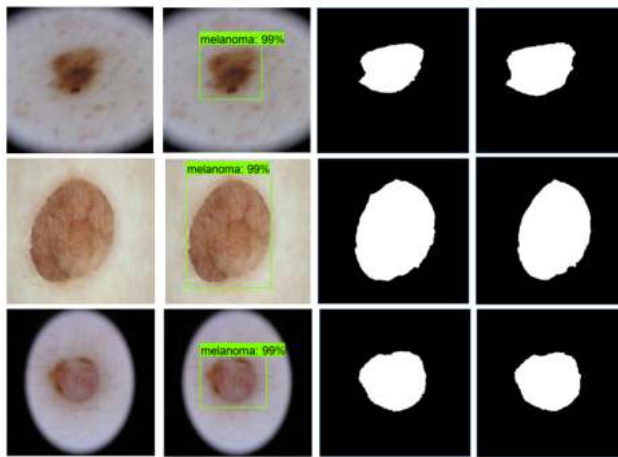


Fig. 5. (a) input image. (b) SSD detected Melanoma lesion. (c) Ground truth Melanoma lesion images. (d) Level set segmentation of Melanoma boundary.

2) *Melanoma Segmentation*: To evaluate the segmentation performance we have computed the average of specificity (SP), sensitivity (SE), accuracy (Ac), Jaccard index (Jc), and dice score (Di) values for all test images on ISIC 2016. On ISIC 2016 our proposed technique achieved an average of SE of 0.83%, SP of 0.98%, and Ac of 0.90%. Similarly, for segmentation, we also calculated average values of Jc and dice as 0.82 and 0.90 respectively for all test samples. The resultant segmented images of ISIC 2016 are shown in the Figure 5(d) which are very similar to the ground truth images shown in the Figure 5(c). Our proposed framework performs good segmentation because of the accurate detection of Melanoma lesion region using SSD. The results of segmentation over ISIC 2016 are shown in the Table. 2.

TABLE II  
PERFORMANCE OF PROPOSED METHOD'S SEGMENTATION RESULTS ON ISIC 2016 DATASET

Dataset	Ac	Di	Jc	SE	SP
ISIC 2016	0.90	0.901	0.82	0.83	0.98

### C. Comparative analysis

1) *Comparisons with state-of-the-art methods*: We also compared the performance of our segmentation results with the state-of-the-art methods. It can be observable from Table 3 that the traditional segmentation methods including, thresholding [15], statistical region split & merge [16], bootstrap learning [17], contextual hypergraph [18], clustering [19], active contours [15], and sparse coding [20] performed lower segmentation results in terms of Jaccard than our proposed method. The FCN and Segnet deep learning approaches performed segmentation and both achieved 0.86 Jc value. In addition [11], RCNN deep learning based also performed good segmentation with 0.93 Jc score which is better than our method. But RCNN generates region proposal which makes the network very complex and computationally expensive. The Level set achieved 0.46 Jc whereas our SSD method combined with Levelset method outperformed the alone levelset method by 36%. The reason behind the excellence performance as compared to other traditional level set method is good localization of melanoma lesion through SSD approach. Furthermore, it automatically excludes some artifacts i.e. ruler markings, clinical charts, black framee which hinders in precise segmenation of melanoma region.

TABLE III  
COMPARISON OF PERFORMANCE OF ISIC 2016 OVER TRADITIONAL  
SEGMENTATION METHODS.

Techniques	Ac	Di	Jc	SP
Adaptive thresholding [15]	0.72	0.56	0.45	0.8
ISO [21]	0.82	0.68	0.56	0.77
Yen thresholding [16]	0.81	0.67	0.58	0.77
Level set active contour [22]	0.7	0.58	0.46	0.79
Statistical region growing [16]	0.73	0.55	0.43	0.76
Bootstrap learning [17]	0.78	0.72	0.57	0.75
Contextual hypergraph [18]	0.83	0.75	0.6	0.78
Sparse coding [20]	0.91	0.8	0.67	0.86
<b>Proposed</b>	<b>0.90</b>	<b>0.901</b>	<b>0.82</b>	<b>0.98</b>

#### IV. CONCLUSION

In our work, we adopted a novel method based on SSD and Level set method for automated Melanoma detection and segmentation by overcoming the ISIC dataset challenges present in dermoscopic images. In comparison with the state-of-the-art object detection models, the SSD model is capable of multi-box detections along with the classification of more than one classes. Therefore the SSD is able to detect several skin diseases, at the same time for an individual patient as well as for multiple patients. To show the robustness of our work we performed results on ISIC 2016 dataset titled "Skin Lesion Analysis towards Melanoma detection". In the future, we may perform the classification task by integrating our proposed Melanoma localization and segmentation task. In addition to that we also plan to generalize our work on other applications in medical imaging field to solve complex segmentation and recognition problems.

#### REFERENCES

- [1] J. D'Orazio, S. Jarrett, A. Amaro-Ortiz, and T. Scott, "UV radiation and the skin," *Int. J. Mol. Sci.*, vol. 14, no. 6, pp. 12222–12248, 2013.
- [2] R. L. Siegel, K. D. Miller, and A. Jemal, "Cancer statistics, 2019.," *CA. Cancer J. Clin.*, vol. 69, no. 1, pp. 7–34, 2019.
- [3] X. Zhang, "Melanoma segmentation based on deep learning," *Comput. Assist. Surg.*, vol. 0, no. 0, pp. 267–277, 2017.
- [4] K. Wolff, "Why is epiluminescence microscopy important?," *Recent Results Cancer Res.*, vol. 160, pp. 125–32, 2002.
- [5] N. Otsu, "Otsu 1979 Otsu threshold method," *IEEE Trans. Syst. Man. Cybern.*, vol. C, no. 1, pp. 62–66, 1979.
- [6] C. Barata, M. Ruela, M. Francisco, T. Mendonca, and J. S. Marques, "Two systems for the detection of melanomas in dermoscopy images using texture and color features," *IEEE Syst. J.*, vol. 8, no. 3, pp. 965–979, 2014.
- [7] A. Wong, J. Scharcanski, and P. Fieguth, "Automatic skin lesion segmentation via iterative stochastic region merging," *IEEE Trans. Inf. Technol. Biomed.*, vol. 15, no. 6, pp. 929–936, 2011.
- [8] S. Osher and J. A. Sethian, "Fronts propagating with curvature-dependent speed: Algorithms based on Hamilton-Jacobi formulations," *J. Comput. Phys.*, vol. 79, no. 1, pp. 12–49, 1988.
- [9] T. F. Chan and L. A. Vese, "Active contours without edges," *IEEE Trans. Image Process.*, vol. 10, no. 2, pp. 266–277, 2001.
- [10] Y. Yuan, M. Chao, and Y. C. Lo, "Automatic Skin Lesion Segmentation Using Deep Fully Convolutional Networks with Jaccard Distance," *IEEE Trans. Med. Imaging*, vol. 36, no. 9, pp. 1876–1886, 2017.
- [11] N. Nida, A. Irtaza, A. Javed, M. H. Yousaf, and M. T. Mahmood, "Melanoma lesion detection and segmentation using deep region based convolutional neural network and fuzzy C-means clustering," *Int. J. Med. Inform.*, vol. 124, pp. 37–48, 2019.
- [12] J. Zou, X. Ma, C. Zhong, and Y. Zhang, "Dermoscopic Image Analysis for ISIC Challenge 2018," pp. 2–5, 2018.

- [13] D. Impiombato et al., "SSD: Single Shot MultiBox Detector Wei," *Nucl. Instruments Methods Phys. Res. Sect. A Accel. Spectrometers, Detect. Assoc. Equip.*, vol. 794, pp. 185–192, 2015.
- [14] G. Hinton, N. Srivastava, and K. Swersky, "Lecture notes: Neural Networks for Machine Learning," Univ. Toronto, 2014.
- [15] M. Silveira et al., "Comparison of segmentation methods for melanoma diagnosis in dermoscopy images," *IEEE J. Sel. Top. Signal Process.*, vol. 3, no. 1, pp. 35–45, 2009.
- [16] M. E. Celebi et al., "Border detection in dermoscopy images using statistical region merging," *Ski. Res. Technol.*, vol. 14, no. 3, pp. 347–353, 2008.
- [17] S. Chen, "Chaotic spread spectrum watermarking for remote sensing images," *J. Electron. Imaging*, vol. 13, no. 1, p. 220, 2004.
- [18] X. Li, Y. Li, C. Shen, A. Dick, and A. Van Den Hengel, "Contextual hypergraph modeling for salient object detection," *Proc. IEEE Int. Conf. Comput. Vis.*, pp. 3328–3335, 2013.
- [19] Z. Liu and J. Zerubia, "Skin image illumination modeling and chromophore identification for melanoma diagnosis," *Phys. Med. Biol.*, vol. 60, no. 9, pp. 3415–3431, 2015.
- [20] B. Bozorgtabar, M. Abedini, R. Garnavi, Sparse coding based skin lesion segmentation using dynamic rule-based refinement, 2016. doi:10.1007/978-3-319-47157-0\_31.
- [21] T. W. Ridler and S. Calvard, Picture Thresholding Using an Iterative Selection Method, vol. 8, 1978.
- [22] C. Li, C. Y. Kao, J. C. Gore, and Z. Ding, "Minimization of region-scalable fitting energy for image segmentation," *IEEE Trans. Image Process.*, vol. 17, no. 10, pp. 1940–1949, 2008.